

# Relativistic electronic dressing in laser-assisted electron-hydrogen collisions. I . Elastic collisions.

Y. Attaourti \*, B. Manaut †

*Laboratoire de Physique des Hautes Energies et d'Astrophysique,  
Faculté des Science Semlalia, Université Cadi Ayyad, Marrakech, BP : 2390, Maroc.*

## Abstract

We study the effects of the relativistic electronic dressing in laser-assisted electron-hydrogen atom elastic collisions. We begin by considering the case when no radiation is present. This is necessary in order to check the consistency of our calculations and we then carry out the calculations using the relativistic Dirac-Volkov states. It turns out that a simple formal analogy links the analytical expressions of the differential cross section without laser and the differential cross section in presence of a laser field

PACS number(s): 34.80.Qb, 12.20.Ds

## 1 Introduction

Recently, the study of relativistic aspects of laser-induced processes has proved necessary particularly as a result of very paramount breakthroughs in laser technology which is capable now to attain considerable ultrahigh intensities which could never have been dreamt of three or four decades ago. Many experiments that have shown a relativistic signature have been recently reported. To name some, the transition between Thomson and Compton scattering inside a very strong laser field was investigated by C.I. Moore, J.P. Knauer and D.D. Meyerhofer [1]. C. Bula et al. [2] performed experiments on non linear Compton scattering at SLAC. Also, there are many other types of laser-assisted processes in which relativistic effects may be important. For instance, the process of emission of very energetic electrons and ions from atomic clusters which are submitted to ultrastrong infrared laser pulses [3]. It is now obvious that the whole apparatus and formalism of the non relativistic quantum collision theory [4] has to be revisited in order to extend known non relativistic results to the relativistic domain. Many theoretical studies of laser-assisted electron-atom collision have been mainly carried out in the non relativistic regime. [5].

In presenting this work, we want to show that the modifications of the relativistic differential cross section corresponding to the elastic collision  $e^- + H(I_{s_{1/2}}) \rightarrow e^- + H(I_{s_{1/2}})$  due to the dressing of

---

\*e-mail: [attaourti@ucam.ac.ma](mailto:attaourti@ucam.ac.ma)

†e-mail: [bmanaut@phea.ucam.ac.ma](mailto:bmanaut@phea.ucam.ac.ma)

the Dirac-Volkov electron, in the presence of an ultraintense laser field can provide many interesting insights concerning the importance and the signatures of the relativistic effects.

In this work, we do not consider very high laser intensities that allow pair creation [6] and focus instead on the domain of intensities that justifies a strong classical electromagnetic potential [7]. The Dirac-Volkov electrons are thus dressed by a strong classical electromagnetic field with circular polarization.

The organization of this paper is as follows :

In section (2) we will present the formalism and establish the expression of the relativistic differential scattering cross section in absence of the laser field. This will serve as a guide and test the consistency of the calculation in presence of the laser field. In section (3), we give the expression of the differential cross section in presence of a laser field with circular polarization and we compare it with the relativistic differential cross section without laser field. We show that a simple formal analogy links these two differential cross sections.

In section (4), we give a brief discussion of the results. In section (5), we give a brief conclusion. Throughout this work, we use atomic units and the abbreviation DCS stands for differential cross section.

## 2 Differential cross section without laser field

In order to recover the relativistic differential cross section without the laser field, we begin by considering the process  $e^- + H(1s_{1/2}) \rightarrow e^- + H(1s_{1/2})$  in the absence of radiation. The (direct) transition amplitude corresponding to this process is :

$$\begin{aligned} S_{fi} &= -i \int_{-\infty}^{+\infty} dt \langle \psi_{p_f}(\mathbf{r}_1, t) \phi_f(\mathbf{r}_2, t) | V_d | \psi_{p_i}(\mathbf{r}_1, t) \phi_i(\mathbf{r}_2, t) \rangle \\ &= -\frac{i}{c} \int d^4x_1 \bar{\psi}_{p_f}(\mathbf{r}_1, t) \gamma^0 \psi_{p_i}(\mathbf{r}_1, t) \langle \phi_f(\mathbf{r}_2) | V_d | \phi_i(\mathbf{r}_2) \rangle \end{aligned} \quad (1)$$

Where  $\psi_p(\mathbf{r}, t) = u(p, s) e^{-ip \cdot x} / \sqrt{2EV}$  is the electron wave functions described by a free Dirac spinor normalized to the volume  $V$  and  $\phi_{i,f}(\mathbf{r}_2)$  are the relativistic wave functions of the hydrogen atom where the index  $i$  for the initial state and the index  $f$  stands for the final state. As we study the elastic excitation by electronic impact, we have  $f = i = (1s_{1/2})$ . The velocity of light is  $c = 137.036$  in atomic units the explicit expression of the wave functions  $\phi(\mathbf{r})$  for the fundamental state (spin up) can be found in [8] and reads in atomic units as :

$$\phi(\mathbf{r}) = \frac{1}{\sqrt{4\pi}} \begin{pmatrix} ig(r) \\ 0 \\ f(r) \cos(\theta) \\ f(r) \sin(\theta) e^{i\phi} \end{pmatrix} \quad (2)$$

with  $g(r)$  given by :

$$g(r) = (2Z)^{\gamma+1/2} \sqrt{\frac{1+\gamma}{2\Gamma(1+2\gamma)}} e^{-Zr} r^{\gamma-1} \quad (3)$$

whereas  $f(r)$  is given by :

$$f(r) = -(2Z)^{\gamma+1/2} \sqrt{\frac{1+\gamma}{2\Gamma(1+2\gamma)}} e^{-Zr} r^{\gamma-1} \left( \frac{1-\gamma}{Z\alpha} \right) \quad (4)$$

To simplify the notation we shall use throughout this work the following abbreviations :

$$g(r) = N_g e^{-Zr} r^{\gamma-1}, \quad f(r) = -g(r) \left( \frac{1-\gamma}{Z\alpha} \right) = N_f e^{-Zr} r^{\gamma-1} \quad (5)$$

In Eq.(1),  $V_d$  is the direct interaction potential :

$$V_d = \frac{1}{r_{12}} - \frac{Z}{r_1} \quad (6)$$

where  $\mathbf{r}_1$  are the electron coordinates and  $\mathbf{r}_2$  are the atomic electron coordinates and  $r_{12} = |\mathbf{r}_1 - \mathbf{r}_2|$ .

The parameter  $\gamma$  appearing in all these equations is :

$$\gamma = \sqrt{1 - Z^2 \alpha^2} \quad (7)$$

It is straight forward to get for the transition amplitude:

$$S_{fi} = -i \frac{1}{\sqrt{2E_i 2E_f} V} \frac{1}{V} 2\pi \delta(E_f - E_i) \bar{u}(p_f, s_f) \gamma^0 u(p_i, s_i) H(\Delta) \quad (8)$$

Where  $\gamma^0$  is given in the standard representation of the Dirac matrices by  $\gamma^0 = \text{diag}(1_2, -1_2)$ . The symbol  $1_2$  denotes the  $2 \times 2$  unit matrice. The argument of the function  $H$  is  $\Delta = |\mathbf{p}_i - \mathbf{p}_f|$ , the momentum transfer. The DCS is given by:

$$\frac{d\sigma}{d\Omega_f} = \frac{|\mathbf{p}_f|}{|\mathbf{p}_i|} \frac{1}{(4\pi c^2)^2} \left( \frac{1}{2} \sum_{s_i, s_f} |\bar{u}(p_f, s_f) \gamma^0 u(p_i, s_i)|^2 \right) |H(\Delta)|^2 \Big|_{E_f=E_i} \quad (9)$$

In Eq.(9), we have summed over the final polarization  $s_f$  and averaged over the initial polarization  $s_i$ . For elastic collisions  $|\mathbf{p}_f| = |\mathbf{p}_i| = |\mathbf{p}|$  so that  $E_i = E_f = E$  and :

$$\frac{1}{2} \sum_{s_i, s_f} |\bar{u}(p_f, s_f) \gamma^0 u(p_i, s_i)|^2 = 4E^2 (1 - \beta^2 \sin^2(\theta/2)) \quad (10)$$

with  $\beta = |\mathbf{p}| \frac{c}{E}$ . The angle  $\theta$  is the scattering angle between the vectors  $\mathbf{p}_i$  and  $\mathbf{p}_f$ . We then have for the unpolarized DCS :

$$\frac{d\sigma}{d\Omega_f} = \frac{1}{(4\pi c^2)^2} 4E^2 (1 - \beta^2 \sin^2(\theta/2)) |H(\Delta)|^2 \Big|_{E_f=E_i} \quad (11)$$

We now turn to the function  $H(\Delta)$  of the momentum transfer which is simply proportional to the Fourier transform of the average (static) potential felt by the incident electron in the field of the hydrogen atom [4]. Performing the various integrals, we get for this Fourier transform :

$$H(\Delta) = 4\pi(N_g^2 + N_f^2)\Gamma(2\gamma + 1) \left( \frac{1}{(2Z)^{2\gamma+1}\Delta^2} - \frac{\sin(2\gamma\phi)}{2\gamma\lambda^{2\gamma}\Delta^3} \right) \quad (12)$$

where the quantities  $\lambda$  and  $\phi$  are :

$$\lambda = \sqrt{(2Z)^2 + \Delta^2} \quad \text{and} \quad \phi = \arctan\left(\frac{\Delta}{2Z}\right) \quad (13)$$

Even if it may not seem so, the function  $H(\Delta)$  is well behaved for the case of forward scattering  $\theta = 0^\circ$  ( recall that  $\Delta = 2|\mathbf{p}_i|\sin(\theta/2)$ ) and has the property :

$$\lim_{\Delta \rightarrow 0} \left( \frac{1}{(2Z)^{2\gamma+1}\Delta^2} - \frac{\sin(2\gamma\phi)}{2\gamma\lambda^{2\gamma}\Delta^3} \right) = \frac{(2\gamma + 1)(2\gamma + 2)}{6(2Z)^{2\gamma+3}} \quad (14)$$

We must of course recover the result in the non relativistic limit ( $\beta \rightarrow 0$  and  $\gamma \rightarrow 1$ ). In that case, the differential cross section is simply given by :

$$\frac{d\sigma}{d\Omega_f} = 4 \frac{(\Delta^2 + 8)^2}{(\Delta^2 + 4)^4} \quad (15)$$

Taking  $\beta \rightarrow 0$  and  $\gamma \rightarrow 1$  (for  $Z=1$ ), one easily recovers from Eq. (11) the above mentioned non relativistic limit.

### 3 The differential cross section in presence of a laser field

We turn to the calculation of the DCS for elastic scattering without exchange in the first Born approximation and in the presence of a laser field. The (direct) transition amplitude in this case is given by :

$$\begin{aligned} S_{fi} &= -i \int_{-\infty}^{+\infty} dt \langle \psi_{q_f}(\mathbf{r}_1, t) \phi_f(\mathbf{r}_2, t) | V_d | \psi_{q_i}(\mathbf{r}_1, t) \phi_i(\mathbf{r}_2, t) \rangle \\ &= -\frac{i}{c} \int d^4x_1 \bar{\psi}_{q_f}(\mathbf{r}_1, t) \gamma^0 \psi_{q_i}(\mathbf{r}_1, t) \langle \phi_f(\mathbf{r}_2) | V_d | \phi_i(\mathbf{r}_2) \rangle \end{aligned} \quad (16)$$

where  $\phi_{i,f}(\mathbf{r}_2)$  are the relativistic wave functions of the hydrogen atom and the functions  $\psi_q(\mathbf{r}_1, t)$  are the Dirac-Volkov solutions normalized to the volume  $V$  :

$$\psi_q(\mathbf{r}, t) = \frac{1}{\sqrt{2QV}} R(q) u(p, s) e^{-is(x)} \quad (17)$$

with :

$$R(q) = R(p) = \left( 1 + \frac{1}{2(k.p)c} k(\phi_1 \cos(\varphi) + \phi_2 \sin(\varphi)) \right) \quad (18)$$

and :

$$S(x) = q.x + \frac{(a_1.p)}{c(k.p)} \sin(\varphi) - \frac{(a_2.p)}{c(k.p)} \cos(\varphi) \quad (19)$$

in the case of a circularly polarized electromagnetic potential such that  $A^\mu = a_1^\mu \cos(\varphi) + a_2^\mu \sin(\varphi)$  with  $k_\mu A^\mu = 0$  (the Lorentz condition) and  $A^2 = a_1^2 = a_2^2 = a^2$ ,  $a_1.a_2 = 0$  and  $k.a_1 = k.a_2 = 0$ . The four-vector  $q^\mu = (Q/c, \mathbf{q})$  is the four-momentum of the electron inside the laser field with wave four-vector  $k^\mu$ .

We have :

$$q^\mu = p^\mu - \frac{a^2}{2(k.p)c^2} k^\mu \quad (20)$$

In Eq(20)  $a^2$  denotes the time-averaged square of the four-vector potential of the laser field. The square of this four-vector is :

$$q_\mu q^\mu = m_*^2 c^2 \quad (21)$$

The parameter  $m_*$  plays the role of an effective mass of the electron inside the electromagnetic field :

$$m_*^2 = 1 - \frac{a^2}{c^4} \quad (22)$$

The factor  $R(q)$  acting on the bispinor  $u$  contains information about the spin-dressing field interaction. Thus, the Dirac-Volkov wave function represents a free-electron wave (containing a field-dependent phase) modulated by a wave generated by the interaction of the spin with the classical single mode field with four-vector potential  $A^\mu$ .

In Eqs. (18,19),  $\varphi = k.x = k_\mu x^\mu = k_0 x^0 - \mathbf{k}.\mathbf{x}$  and we use throughout this work the notations and conventions of Bjorken and Drell [8]. Proceeding along the lines of standard calculations in QED [8], one has for the DCS :

$$\frac{d\sigma}{d\Omega_f} = \sum_{s=-\infty}^{\infty} \frac{d\sigma^{(s)}}{d\Omega_f} \quad (23)$$

where  $\frac{d\sigma^{(s)}}{d\Omega_f}$  is the DCS corresponding to the net exchange of  $s$  photons and reads :

$$\frac{d\sigma^{(s)}}{d\Omega_f} = \frac{1}{(4\pi c)^2} \frac{|\mathbf{q}_f|}{|\mathbf{q}_i|} \left( \frac{1}{2} \sum_{s_i s_f} |M_{fi}^{(s)}|^2 \right) |H^{(s)}(\Delta^{(s)})|^2 \Bigg|_{Q_f=Q_i+sw} \quad (24)$$

Here  $\Delta_s = |\mathbf{q}_i + s\mathbf{k} - \mathbf{q}_f|$  is the momentum transfer with the net exchange of  $s$  photons. The quantity  $(\frac{1}{2} \sum_{s_i s_f} |M_{fi}^{(s)}|^2)$  is the electronic contribution to the differential cross section  $\frac{d\sigma^{(s)}}{d\Omega}$  and has already been determined in a previous work [9]. We simply quote the final result:

$$\begin{aligned} & \frac{1}{2} \sum_{s_i s_f} |M_{fi}^{(s)}|^2 \\ &= \frac{2}{c^2} \{ J_s^2(z)A + (J_{s+1}^2(z) + J_{s-1}^2(z))B \\ &+ (J_{s+1}(z)J_{s-1}(z))C + J_s(z)(J_{s-1}(z) + J_{s+1}(z))D \} \end{aligned} \quad (25)$$

where the argument  $z$  of the Bessel functions is given by  $z = \sqrt{\alpha_1^2 + \alpha_2^2}$  and  $\alpha_1$  and  $\alpha_2$  are such that :

$$\alpha_1 = \frac{1}{c} \left\{ \frac{a_1 \cdot p_i}{k \cdot p_i} - \frac{a_1 \cdot p_f}{k \cdot p_f} \right\}, \quad \alpha_2 = \frac{1}{c} \left\{ \frac{a_2 \cdot p_i}{k \cdot p_i} - \frac{a_2 \cdot p_f}{k \cdot p_f} \right\} \quad (26)$$

The coefficients  $A$ ,  $B$ ,  $C$  and  $D$  are respectively given by :

$$\begin{aligned} A &= c^4 - (q_f \cdot q_i)c^2 + 2Q_f Q_i - \frac{a^2}{2} \left( \frac{(k \cdot q_f)}{(k \cdot q_i)} + \frac{(k \cdot q_i)}{(k \cdot q_f)} \right) + \frac{a^2 \omega^2}{c^2 (k \cdot q_f)(k \cdot q_i)} ((q_f \cdot q_i) - c^2) + \\ & \frac{(a^2)^2 \omega^2}{c^4 (k \cdot q_f)(k \cdot q_i)} + \frac{a^2 \omega}{c^2} (Q_f - Q_i) \left( \frac{1}{(k \cdot q_i)} - \frac{1}{(k \cdot q_f)} \right) \end{aligned} \quad (27)$$

$$\begin{aligned} B &= -\frac{(a^2)^2 \omega^2}{2c^4 (k \cdot q_f)(k \cdot q_i)} + \frac{\omega^2}{2c^2} \left( \frac{(a_1 \cdot q_f)(a_1 \cdot q_i)}{(k \cdot q_f)(k \cdot q_i)} + \frac{(a_2 \cdot q_f)(a_2 \cdot q_i)}{(k \cdot q_f)(k \cdot q_i)} \right) - \frac{a^2}{2} + \\ & \frac{a^2}{4} \left( \frac{(k \cdot q_f)}{(k \cdot q_i)} + \frac{(k \cdot q_i)}{(k \cdot q_f)} \right) - \frac{a^2 \omega^2}{2c^2 (k \cdot q_f)(k \cdot q_i)} ((q_f \cdot q_i) - c^2) + \\ & \frac{a^2 \omega}{2c^2} (Q_f - Q_i) \left( \frac{1}{(k \cdot q_f)} - \frac{1}{(k \cdot q_i)} \right) \end{aligned} \quad (28)$$

$$\begin{aligned} C &= \frac{\omega^2}{c^2 (k \cdot q_f)(k \cdot q_i)} (\cos(2\phi_0) \{ (a_1 \cdot q_f)(a_1 \cdot q_i) - (a_2 \cdot q_f)(a_2 \cdot q_i) \} + \\ & \sin(2\phi_0) \{ (a_1 \cdot q_f)(a_2 \cdot q_i) + (a_1 \cdot q_i)(a_2 \cdot q_f) \}) \end{aligned} \quad (29)$$

$$\begin{aligned} D &= \frac{c}{2} \left( (\dot{A} \cdot q_i) + (\dot{A} \cdot q_f) \right) - \frac{c}{2} \left( \frac{(k \cdot q_f)}{(k \cdot q_i)} (\dot{A} \cdot q_i) + \frac{(k \cdot q_i)}{(k \cdot q_f)} (\dot{A} \cdot q_f) \right) + \\ & \frac{\omega}{c} \left( \frac{Q_i (\dot{A} \cdot q_f)}{(k \cdot q_f)} + \frac{Q_f (\dot{A} \cdot q_i)}{(k \cdot q_i)} \right) \end{aligned} \quad (30)$$

The function  $H^{(s)}(\Delta_s)$  is now given by :

$$H^{(s)}(\Delta_s) = 4\pi(N_g^2 + N_f^2)\Gamma(2\gamma + 1) \left( \frac{1}{(2Z)^{2\gamma+1}(\Delta_s)^2} - \frac{\sin(2\gamma\phi_s)}{2\gamma\lambda_s^{(2\gamma)}(\Delta_s)^3} \right) \quad (31)$$

with  $\lambda_s = \sqrt{(2Z)^2 + (\Delta_s)^2}$  and  $\phi_s = \arctan(\Delta_s/2Z)$ . Once again, the function  $H^{(s)}(\Delta_s)$  is well behaved for the forward scattering which corresponds to  $s = 0$ . When no radiation field is present, all Bessel functions vanish except for  $s = 0$ : We have  $J_s(z = 0) = \delta_{s0}$  and in this case, the result reduces to the unpolarized DCS given in Eq. (11)

## 4 Results and discussions

The kinematics of the process is that given in [9] and we maintain the same choice for the laser angular frequency, that is  $w = 0.043$  which corresponds to a near-infrared neodymium laser.

### 4.1 The Nonrelativistic regime

In the limit of low electron kinetic energy and moderate field strength, typically an electron kinetic energy  $W = 100 \text{ a.u.}$  and a field strength  $\varepsilon = 0.05 \text{ u.a.}$ , it is easy to see that the effects of the additional spin terms and the dependence of  $q^\mu$  on the spatial orientation of the electron momentum due to  $(k.p)$  are expected to be small. For  $W = 100 \text{ a.u.}$  and  $\varepsilon = 0.05 \text{ u.a.}$ , some angles  $\theta(\mathbf{q}_i, \mathbf{q}_f)$  and  $\theta(\mathbf{p}_i, \mathbf{p}_f)$  are given in Table.1 and this shows indeed that the dependence of  $q^\mu$  (and hence of  $\mathbf{q}$ ) on the spatial orientation of the electron momentum is indeed small in the nonrelativistic regime.

In Fig. (1), we compare the non relativistic DCS given by Eq. (15) and the relativistic DCS given by Eq. (11) as functions of the scattering angle  $\theta(\mathbf{p}_i, \mathbf{p}_f)$  in absence of the laser field. As expected, in the nonrelativistic limit, there is only a small difference between these two cross sections and we see that this difference becomes more pronounced for the case of forward scattering. For large angle scattering, there is almost no difference between the nonrelativistic calculations and the relativistic calculations. In Fig. (2), instead of plotting  $\left(\frac{d\sigma}{d\Omega_f}\right)_{NR}$  and  $\left(\frac{d\sigma}{d\Omega_f}\right)_{REL}$  as functions of the scattering angle, we use the angular coordinates  $(\theta_i, \phi_i)$  of  $\mathbf{p}_i$  and  $(\theta_f, \phi_f)$  of  $\mathbf{p}_f$  to plot the angular dependence of the two DCSs as functions of  $\theta_f$ , the angle between  $\mathbf{p}_f$  and the  $Oz$  axis. This will serve as a consistency check of our next calculations in presence of an electromagnetic potential circularly polarized and whose wave-vector points in the  $Oz$  direction. We have chosen a geometry where  $\theta_i = \phi_i = 45^\circ$  and the angle  $\theta_f$  varies from  $0^\circ$  to  $180^\circ$  with  $\phi_f = 90^\circ$ . The relativistic parameter  $\gamma_{rel} = 1/\sqrt{1 - \beta^2}$  is equal to 1.0053 which corresponds to an electron kinetic energy equal to  $100 \text{ u.a.} \simeq 2.721 \text{ keV}$ . The first observation to be made is that in the non relativistic regime, the non relativistic DCS is very close to the relativistic one, which was to be expected. Also, there a peak in the vicinity of  $\theta_f = 35^\circ$ .

In Fig. (3), we compare the relativistic summed DCS with and without laser field for the net exchange of  $\pm 100$  photons. As one can see, the laser field gives rise to important modifications of

the DCS. for this collision geometry, several hundred photons can be exchanged even in the case of a moderate laser intensity of  $8.75 \times 10^{13} \text{ W/cm}^2$ . In Fig. (4), the net exchange of  $\pm 200$  photons shows that the DCS with laser field approaches the DCS without laser field and we have almost two indistinguishable curves in the case of the net exchange  $\pm 300$  photons as one can see in Fig. (5).

It is also important to compare the relativistic DCS  $\left(\frac{d\sigma^{(s)}}{d\Omega}\right)$  corresponding to the net exchange of  $s$  photons where only the electronic dressing term is taken into account, with the corresponding non relativistic DCS. Working with the nonrelativistic Volkov states, one easily gets for the non relativistic case :

$$\frac{d\sigma^{B_1,s}}{d\Omega_f} = \frac{|\mathbf{p}_f(s)|}{|\mathbf{p}_i|} J_s^2 \left( \frac{|A|}{cw} |\mathbf{p}_i - \mathbf{p}_f(s)| \right) \times \frac{d\sigma^{B_1,F,F}}{d\Omega_f} \quad (32)$$

where the first-Born DCS is given by Eq. (15) and corresponds to the field free case. In Fig. (6), we compare the non relativistic and relativistic DCS for an exchange of  $\pm 100$  photons and for a geometry where  $\theta_i = \phi_i = 45^\circ$  and  $\phi_f = 90^\circ$ . In the non relativistic regime, both approaches give similar results particularly for large angle scattering namely  $\theta_f \geq 45^\circ$ . In Fig. (7), and for the same values of the angular parameters, one cannot distinguish the two curves in the case of an exchange of  $\pm 300$  photons above  $70^\circ$ . Beyond this value, the non relativistic DCS is lower than the relativistic one. In Fig. (8), the DCSs for the absorption of one photon are shown and there is a qualitative difference between the two approaches. Indeed, we have already mentioned that there is a peak in the vicinity of  $\theta_f = 35^\circ$  when we have plotted the two DCS as functions of  $\theta_f$ . This peak is peculiar to the geometry chosen and the relativistic DCS corresponding to the absorption of one photon is peaked for  $\theta_f \simeq 35^\circ$  whereas the non relativistic one is peaked at about  $\theta_f = 30^\circ$ . One explanation that can be given to this difference is that spin-effects as well as relativistic electronic dressing that are fully taken into account in the relativistic treatment influence the location of such peaks. This is another reason that gives a strong motivation to study relativistic effects in laser-assisted electron-atom collisions. Experimentalists need to have theoretical predictions that will enable them to focus on a particular direction. Of course, this is only a modification. due to the relativistic electronic dressing. To be complete, we shall present very soon, a treatment that takes into account the relativistic dressing of the atomic system by the strong radiation field. In Fig. (9), and for the same values of angular parameters, the DCSs for the emission of one photon are given and as expected there is a complete analogy between the process of absorption and emission. In fact, these two processes give the same values for the DCSs.

## 4.2 The relativistic regime

In the limit of high electron kinetic energy and strong field strength, typically an electron kinetic energy  $W = c^2 a.u$  and a field strength  $\varepsilon = 1.00 a.u$ , the effects of the additional spin terms and



the dependence of  $q^\mu$  on the spatial orientation of the electron momentum due to  $(k.p)$  begin to be noticeable. For these values of  $W$  and  $\varepsilon$ , some cos of angle  $\theta(\mathbf{q}_i, \mathbf{q}_f)$  and  $\theta(\mathbf{p}_i, \mathbf{p}_f)$  are given in Table.2 and this shows indeed that the dependence of  $q^\mu$  (and hence of  $\mathbf{q}$ ) on the spatial orientation of the electron momentum is not negligible in the relativistic regime.

In Fig. (10), the non relativistic DCS is compared to the relativistic DCS as functions of the scattering angle  $\theta$  (not to be confused with the angle  $\theta_f$ ). The nonrelativistic formalism is no longer applicable since there is now a net difference between the DCS given by Eq. (11) and the DCS given by Eq. (15) particularly for small angles. Indeed, for the case of forward scattering,  $\left(\frac{d\sigma}{d\Omega}\right)_{NR} = 1$  while  $\left(\frac{d\sigma}{d\Omega}\right)_R \simeq 4$  and the difference between the DCS remains noticeable up to  $\theta = 1.5^\circ$ . For large angles, both approaches give nearly the same results. In Fig. (11), we compare the non relativistic DCS and the relativistic DCS without laser field as functions of the angle  $\theta_f$ . Again, these two DCS present both a peak in the vicinity of  $\theta_f \simeq 35^\circ$ . It is clear that the non relativistic formalism is no longer applicable as we have considered now a relativistic parameter  $\gamma_{rel} = 2$ , with corresponds to an electron kinetic energy of about  $0.511 \text{ Mev}$ . It is a fully relativistic regime and we show in Fig. (12) the DCS with (dashed line ) and without (dotted line ) laser field for the net exchange of  $\pm 3500$  photons. Even in this case, the DCS with laser field is almost smeared out and one has to go up to a very large number of photon exchange to recover the relativistic DCS without laser field. Unfortunately, and due to a lack of high speed computing facilities, we cannot present for the time being a complete analysis of the relativistic and the ultrarelativistic regime. However this will be done in forthcoming paper. Now, we compare the DCSs in the relativistic regime, for the relativistic parameter  $\gamma = 2$ . In Fig. (13), we compare the summed DCS relativistic and non relativistic where there is an exchange of  $\pm 500$  photons. The values of the nonrelativistic DCS is almost halved with regard to the relativistic DCS. In Fig (14), we show the angular distribution of the two DCSs for the process of the absorption of one photon. For the relativistic DCS, there is an appearance of three peaks one located in the vicinity of  $\theta_f = 22.5^\circ$  and double peak in the interval  $(40^\circ, 45^\circ)$  while for the non relativistic DCS, there is a double peak in the vicinity of  $33^\circ$ . We also have the same qualitative result that the non relativistic DCS is almost halved with regard to the relativistic DCS for the process of absorption of one photon. In Fig. (15), we present the same result but for the process of emission of one photon. The values of the DCS are exactly the same as that of the absorption process.

Finally, in Fig. (16), we give the envelope of the differential cross section as a function of the energy transfer  $Q_f - Q_i$  for the non relativistic regime. The final energy-spectrum is not symmetric around the elastic peak.

## 5 Conclusion

In this work, we have studied the effect of the relativistic electronic dressing in laser-assisted electron-hydrogen elastic collisions. To our knowledge, this is the first time that such a calculation has been carried out at this level. Even if the formalism may seem heavy and complicated, we have (using the case with no laser field as a guide ) checked every step of our calculations. What emerges is that the relativistic electronic dressing reduces considerably the magnitude of the DCS. We must sum the DCS given by Eq. (23) over a very large number of photon in order to get the same order of magnitude as that of the DCS given by Eq. (11). Of course, a more sophisticated approach is needed in order to have a complete treatment of this relativistic process. The relativistic generalization of the method due to F.W. Byron and C.J. Joachain [10] which takes into account the atomic dressing will be presented in a separated paper. These authors and others [11] have show that in the non relativistic regime, the dressing of atomic states can give rise to very important modifications of the DCS. The case of inelastic collisions will be published very soon. The non relativistic treatment of laser-assisted electron atom collisions taking into account both the electronic dressing and the atomic dressing has been studied by many authors [12]. All agree that at least in the nonrelativistic regime, the effects of atomic dressing can modify the behaviour of the DCS. The study of the relativistic electronic dressing in laser-assisted inelastic collisions will be sent very soon to the Los Alamos web site xxx.lanl.org. Recently, some authors ([13],[14]) have used the strong field approximation (SFA) to study the photoionization of hydrogen by electron impact. Work is in progress to present a more rigorous approach.

## Acknowledgments

One of us (Y. Attaourti) dedicates the present work to his Teacher and great Master, Prof C.J. Joachain (Université Libre de Bruxelles, Belgium), one of the most outstanding physicist in the field of atomic collision theory who has recently retired and to Prof F. Brouillard (Université Catholique de Louvain, Belgium) , a down-to-earth physicist and a very kind human being.

## References

- [1] C.I. Moore, J.P. Knauer, and D.D. Meyerhofer, *phys.Rev.lett.*, **74**, 2953, (1995).
- [2] C. Bula et al, *Phys. Rev.lett.* **76**, 3116 (1996).
- [3] Y.L. Shao et al, *Nature London*) **386**, 54, (1997).

- [4] C.J. Joachaine, *Quantum collision Theory*, 3rd ed. (Elsevier Science,1983).
- [5] F.V. Bunkin and M.V. Fedrov, Soviet. Phys. JETP **22**, 844 (1966), N.M. Kroll and K.M. Watson, Phys. Rev. A **8**, 804 (1973).
- [6] F.V. Harteman and A.K. Kerman, Phys. Rev. Lett **76**, 624 (1996); F. V. Harteman and N.C. Luhmann, *ibid*, **74**, 1107, (1995).
- [7] C. Zsymanowski, V. Véniard, R. Taïeb, A. Maquet and C.H. Keitel, Phys. rev A, **56**, 3846, 1997.
- [8] J. D. Bjorken and Drell, *Relativistic Quantum Mechanics* (Mac Graw Hill,New York, 1964); C. Itzykson and J-B Zuber, *Quantum field Theory* (Mac Graw Hill,New York,1985).
- [9] Y. Attaourti, B. Manaut, M. Chabab, hep-ph/0207200.
- [10] F. W. Bayron, Jr and C.J. Joachain, J. Phys. B**17**, L295, (1984)
- [11] H. Krüger and M.Schulz, J. Phys. B**9**, 1899, (1976); A. D. Gazazian, J. Phys. B**9**,3197 (1976); N.K. Rahman and F.H.M. Faysal, J. Phys. B **B11**, 2003, (1978); M.J. Coneely and S. Geltman, J. Phys B**14**,4847, (1981); A. lami and N.K. Rahman, J; Phys, **B16**, L201 (1984); S. Jetzke, F.H.M. Faysal, R. Hippler and O.H. Lutz, Zeit. Phys, **A315**, 271, (1984).
- [12] P. Francken and C.J. Joachain, Phys. Rev **A35**, 1590, (1987); A. Dubois, A. Maquet et S.Jetzke, Phys. Rev A**34**, 1888(1986), P. Francken, Y. Attaourti, and C.J. Joachain, Phys. Rev A **38**, (1988).
- [13] H. R. Reiss, J. Opt. Soc. Am. **B7**, 574 (1990).
- [14] D.P. Crawford and H. R. Reiss, Phys. Rev. **A50**, 1844, 1994.

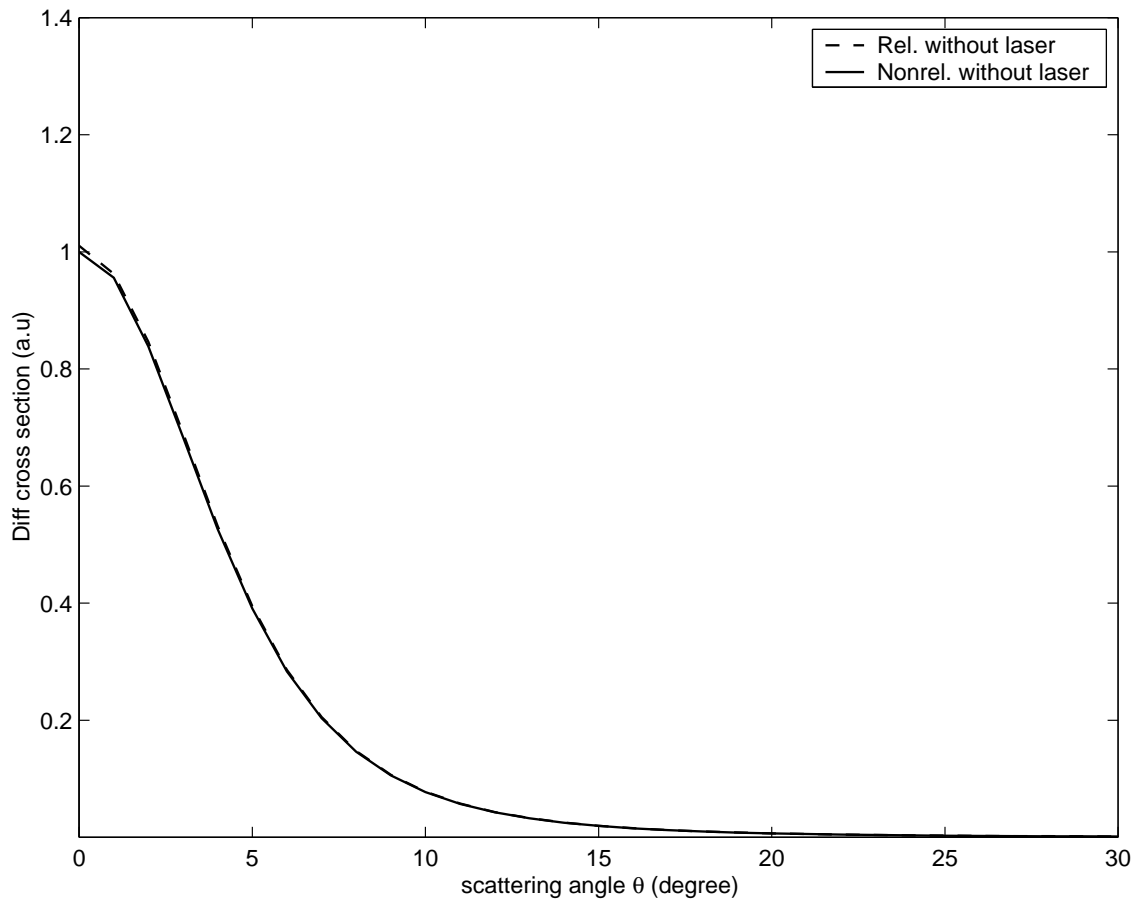


Figure 1: Comparison between the nonrelativistic DCS and the relativistic DCS as functions of the scattering angle ( $\theta$ ) varying from  $0^\circ$  to  $30^\circ$ , without taking into account the spherical coordinates of  $(p_i, p_f)$ ; the curves are perfectly confounded

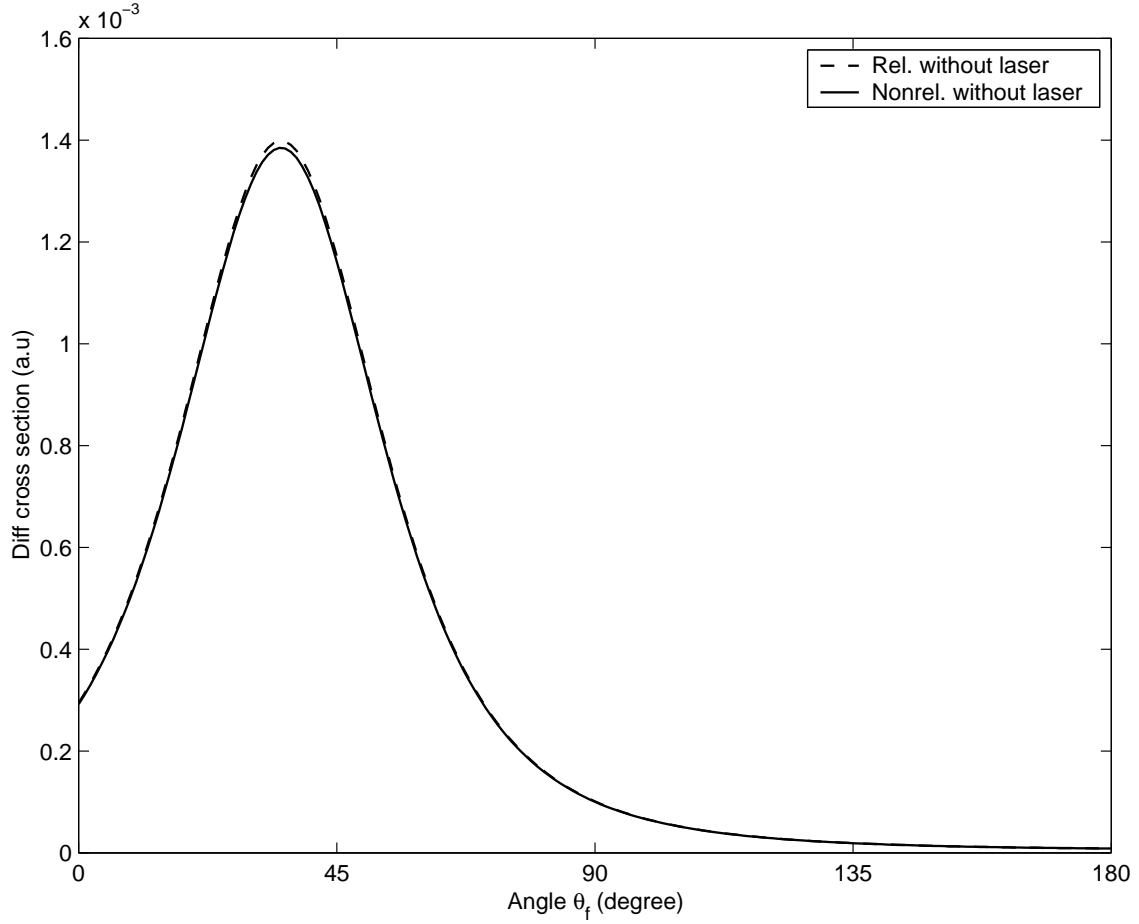


Figure 2: Comparison in the nonrelativistic regime, between the nonrelativistic DCS and the relativistic DCS as functions of  $(\theta_f)$  the angle between  $\mathbf{p}_f$  and the  $Oz$  axis. The parameters are  $\gamma = 1.0053 a.u.$ ,  $\varepsilon = 0.05 a.u.$  and  $w = 0.043 a.u.$ . The geometry chosen is  $\theta_i = \phi_i = 45^\circ$  where  $\theta_f$  varying from  $0^\circ$  to  $180^\circ$  with  $\phi_f = 90^\circ$

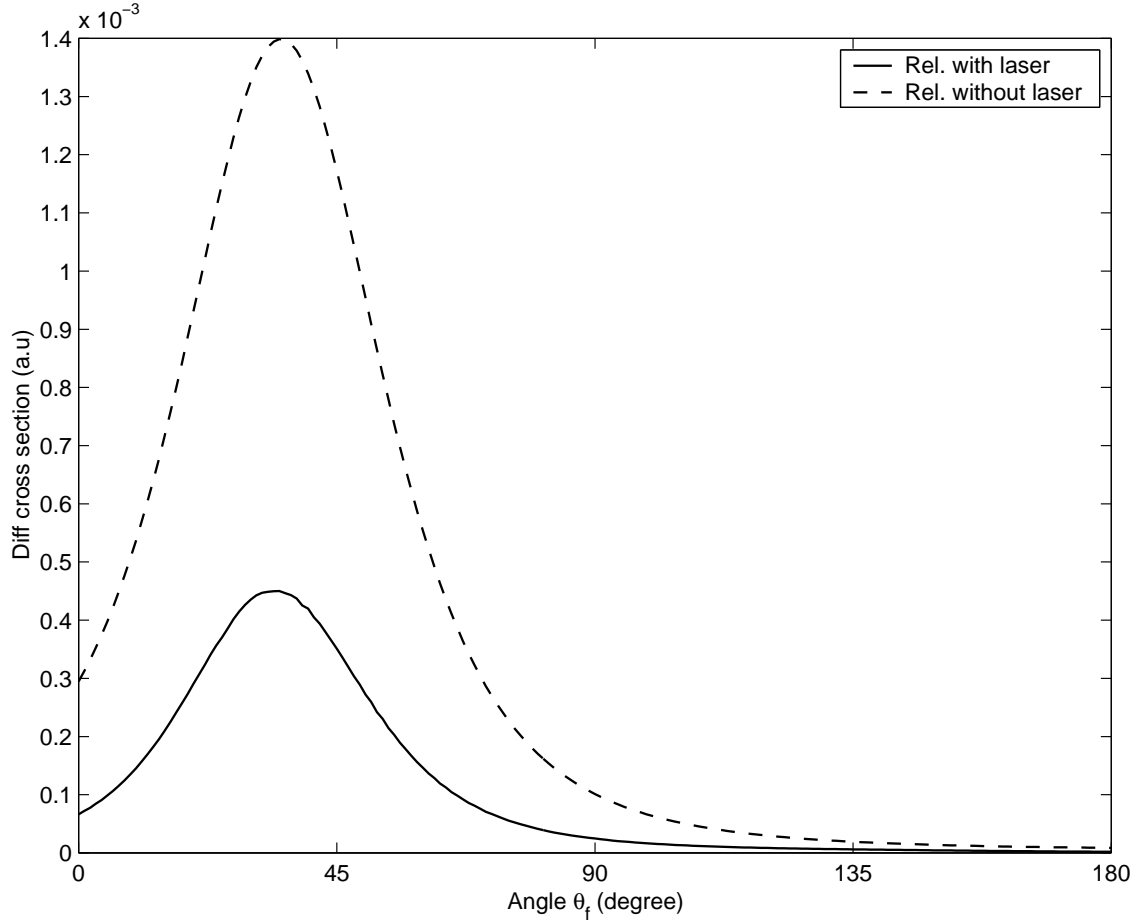


Figure 3: Comparison in the nonrelativistic regime, between the relativistic DCS with laser and the relativistic DCS without laser for the exchange of  $\pm 100$  photons. The parameters are  $\gamma = 1.0053 a.u.$ ,  $\varepsilon = 0.05 a.u.$  and  $w = 0.043 a.u.$ . The geometry chosen is  $\theta_i = \phi_i = 45^\circ$  where  $\theta_f$  varying from  $0^\circ$  to  $180^\circ$  with  $\phi_f = 90^\circ$

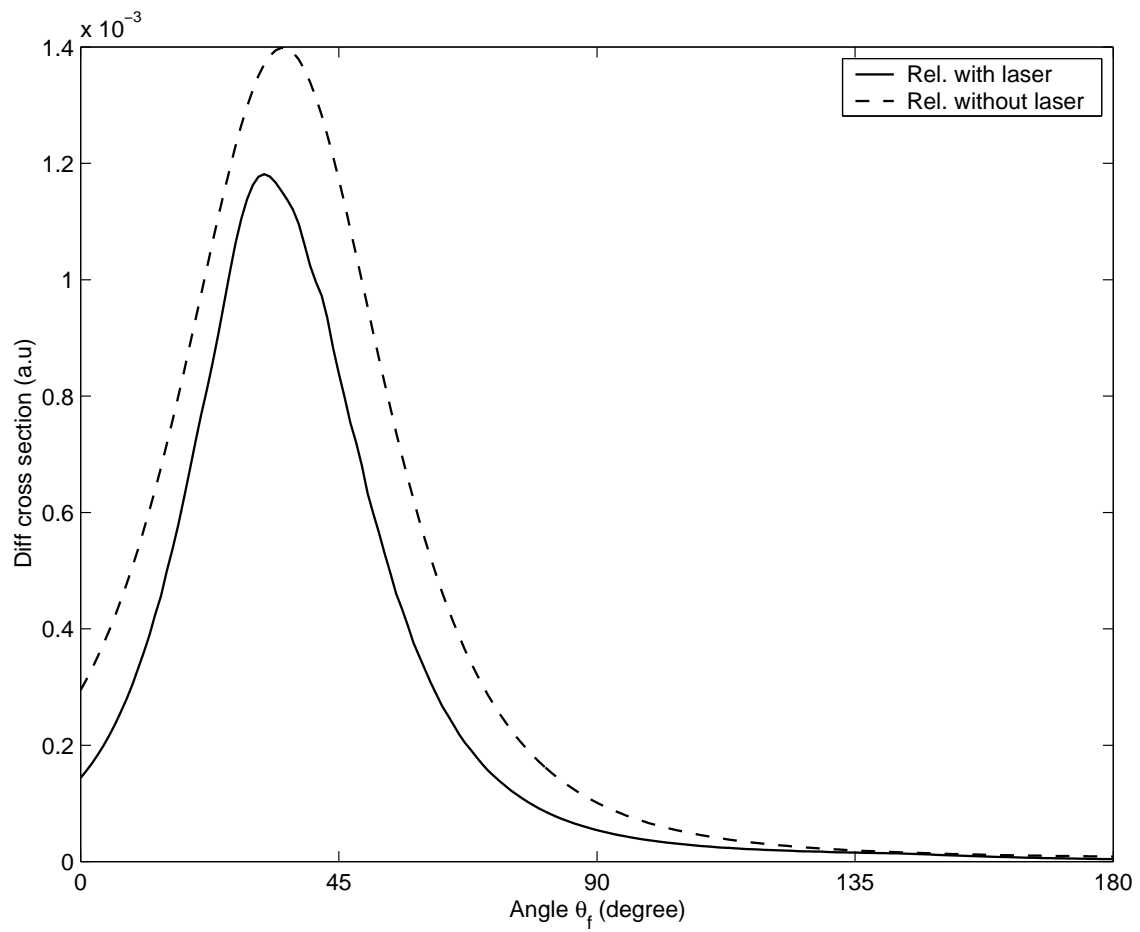


Figure 4: Same as Fig. 3 but for the exchange of  $\pm 200$  photons.

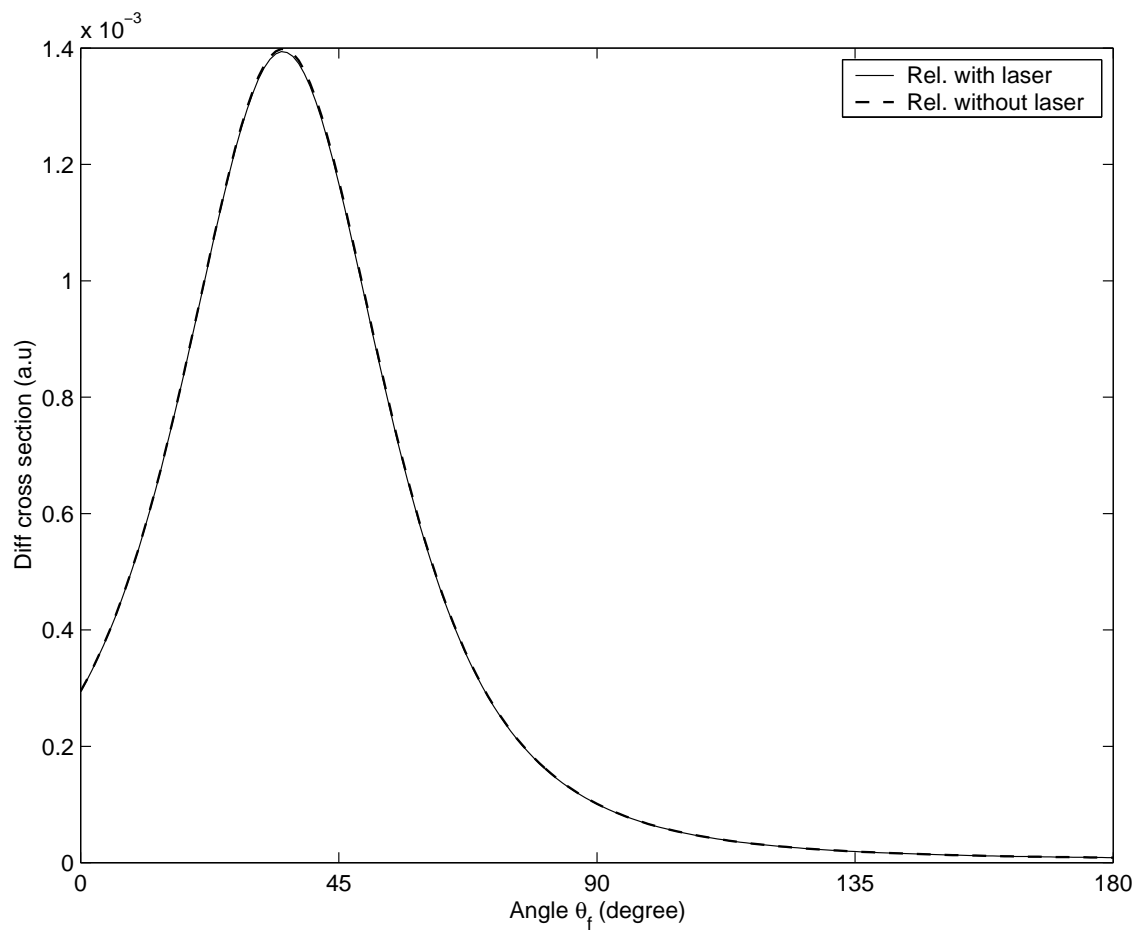


Figure 5: Same as the last figure but for an exchange of  $\pm 300$  photons. The curves are indistinguishable.



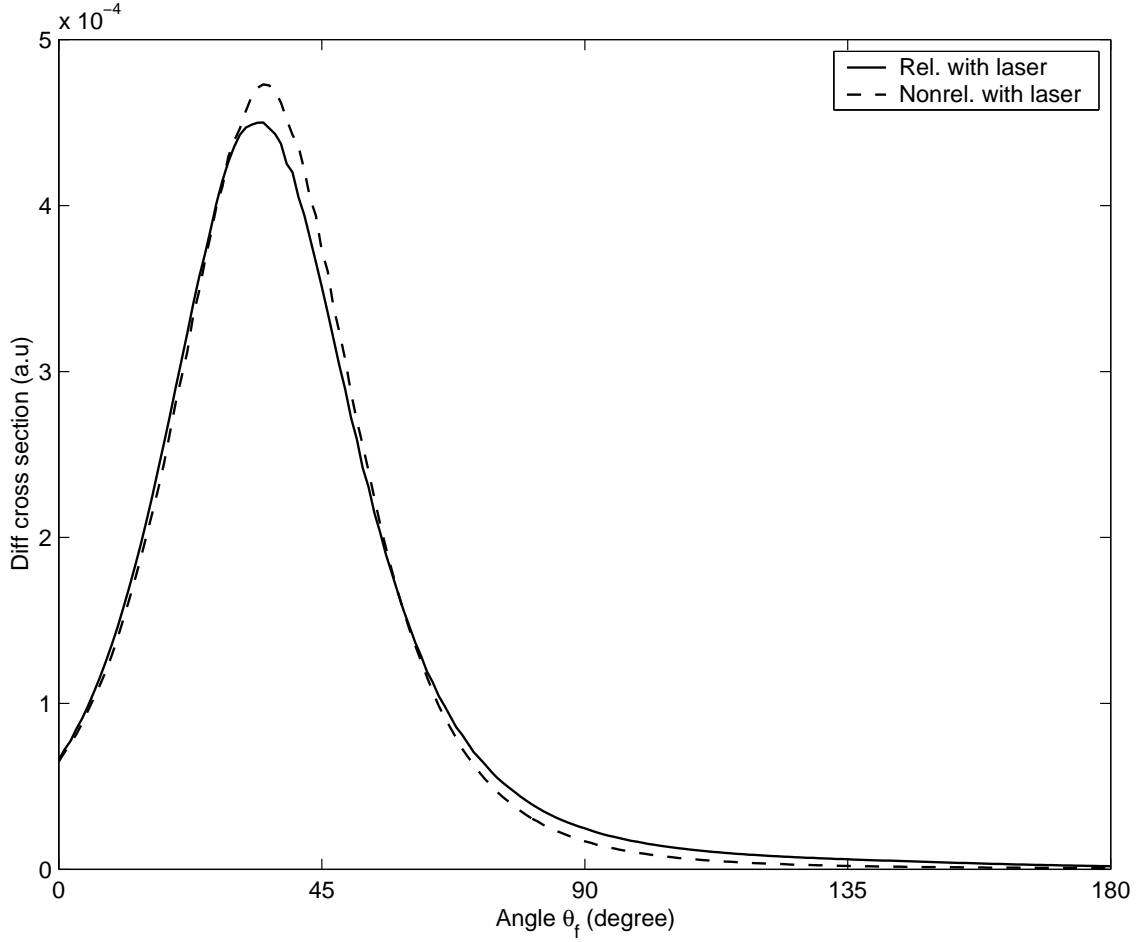


Figure 6: Comparison between the relativistic DCS with laser and the nonrelativistic DCS with laser for an exchange of  $\pm 100$  photons. The parameters are  $\gamma = 1.0053 a.u.$ ,  $\varepsilon = 0.05 a.u.$ ,  $w = 0.043 a.u.$ . The geometry chosen is  $\theta_i = \phi_i = 45^\circ$  where  $\theta_f$  varying from  $0^\circ$  to  $180^\circ$  with  $\phi_f = 90^\circ$

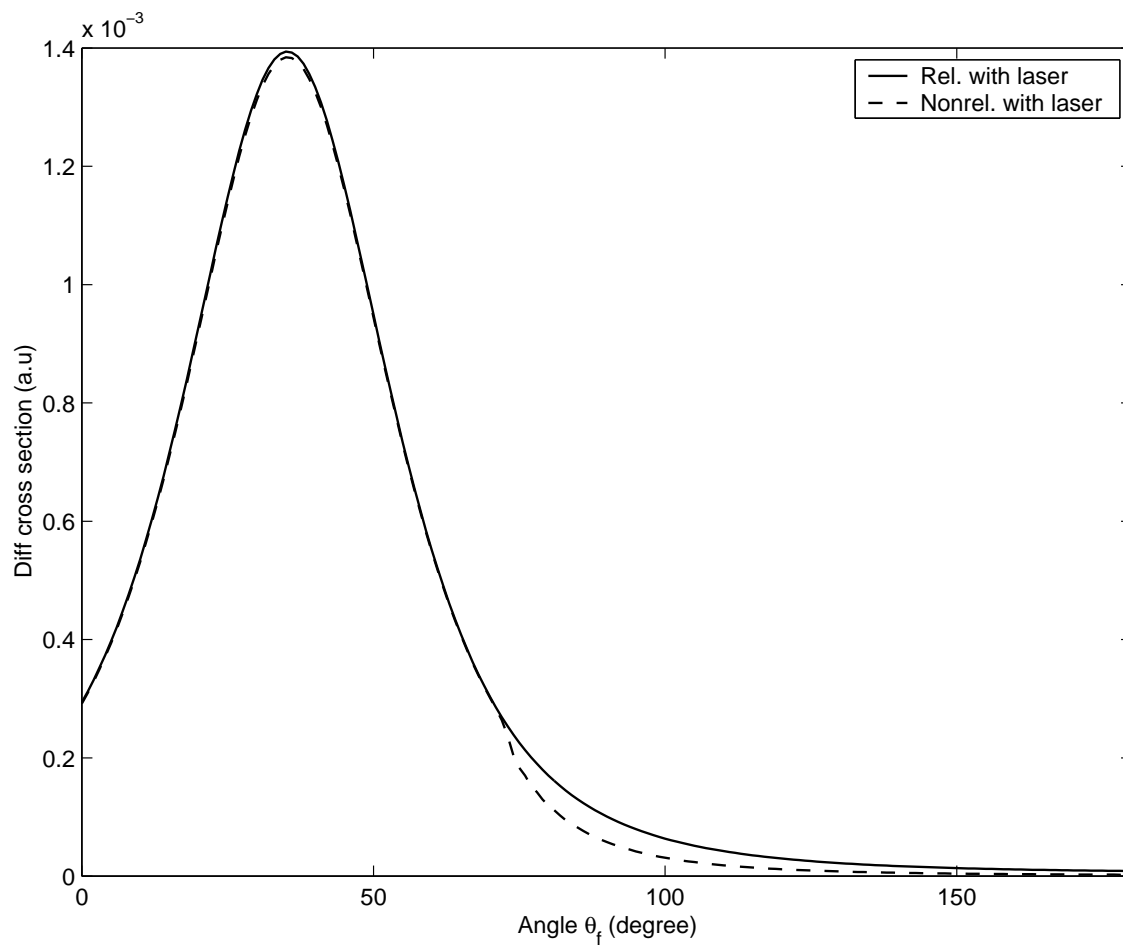


Figure 7: Same as the last Figure but for an exchange of  $\pm 300$  photons. The curves are nearly indistinguishable

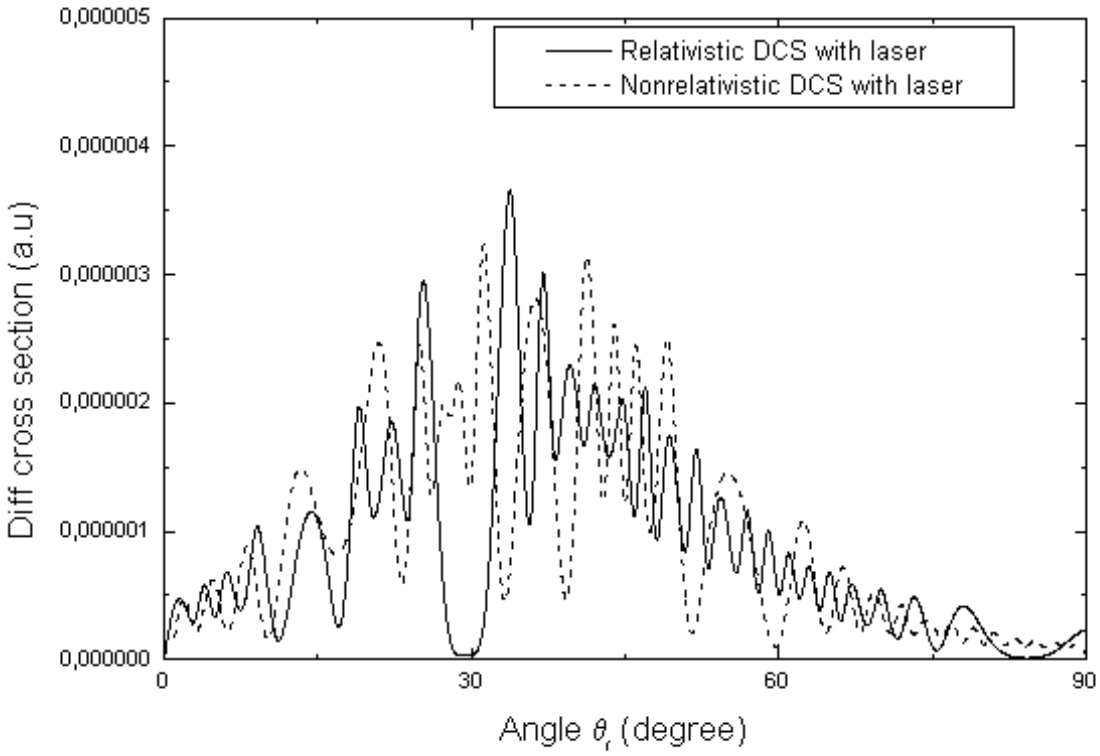


Figure 8: Comparison in the nonrelativistic regime between the relativistic DCS with laser and the nonrelativistic DCS with laser for absorption of one photon. The geometry chosen is  $\theta_i = \phi_i = 45^\circ$  where  $\theta_f$  varying from  $0^\circ$  to  $90^\circ$  with  $\phi_f = 90^\circ$ . The parameters are ( $\gamma = 1.0053 a.u.$ ,  $\varepsilon = 0.05 a.u$  and  $w = 0.043 a.u$ )

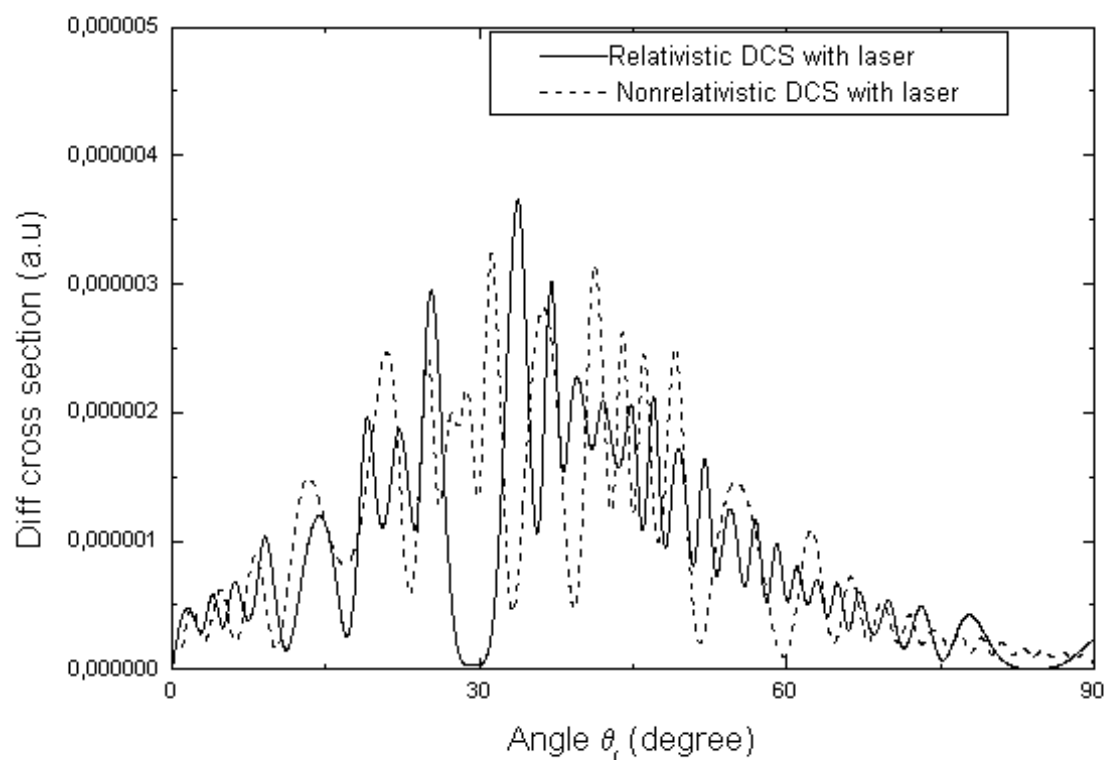


Figure 9: Comparison between the relativistic DCS with laser and the nonrelativistic DCS with laser for the emission of one photon, The parameters are  $\gamma = 1.0053 a.u.$ ,  $\varepsilon = 0.05 a.u.$ ,  $w = 0.043 a.u.$ . The geometry chosen is  $\theta_i = \phi_i = 45^\circ$  where  $\theta_f$  varying from  $0^\circ$  to  $90^\circ$  with  $\phi_f = 90^\circ$

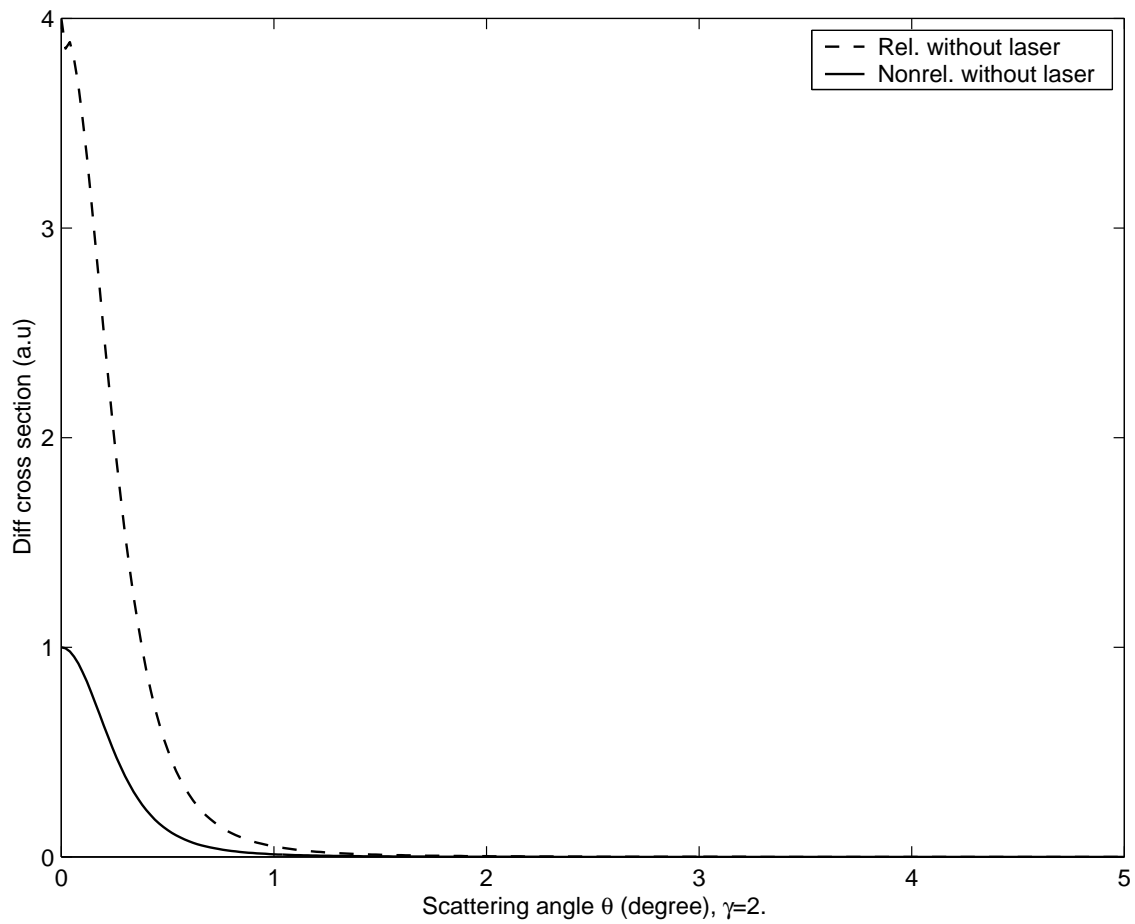


Figure 10: Comparison between the nonrelativistic DCS and the relativistic DCS as functions of the scattering angle ( $\theta$ ) varying from  $0^\circ$  to  $5^\circ$

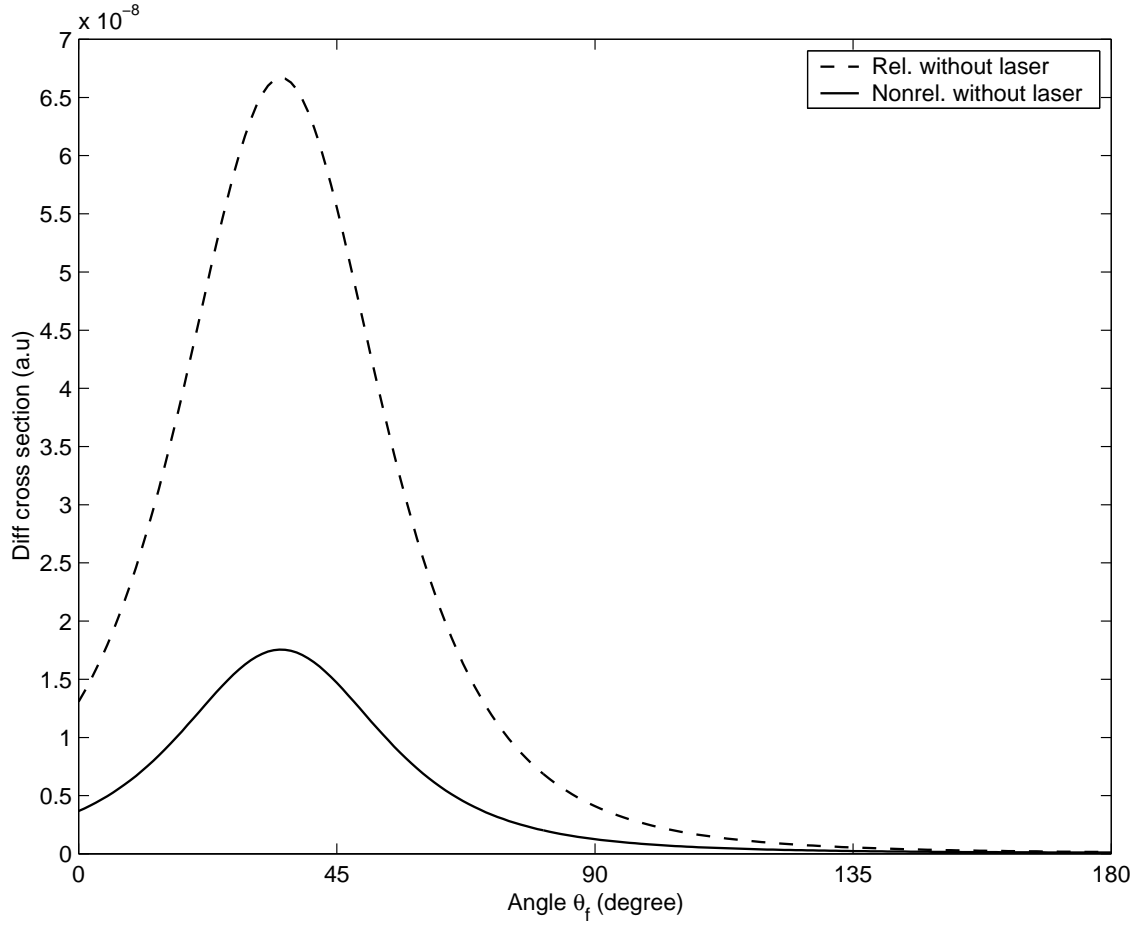


Figure 11: Comparison in the relativistic regime ( $\gamma = 2 a.u.$ ,  $\varepsilon = 1 a.u.$  and  $w = 0.043 a.u.$ ) between the nonrelativistic DCS and the relativistic DCS as functions of  $(\theta_f)$  the angle between  $\mathbf{p}_f$  and the  $Oz$  axis. The geometry chosen is  $\theta_i = \phi_i = 45^\circ$  where  $\theta_f$  varies from  $0^\circ$  to  $180^\circ$  with  $\phi_f = 90^\circ$

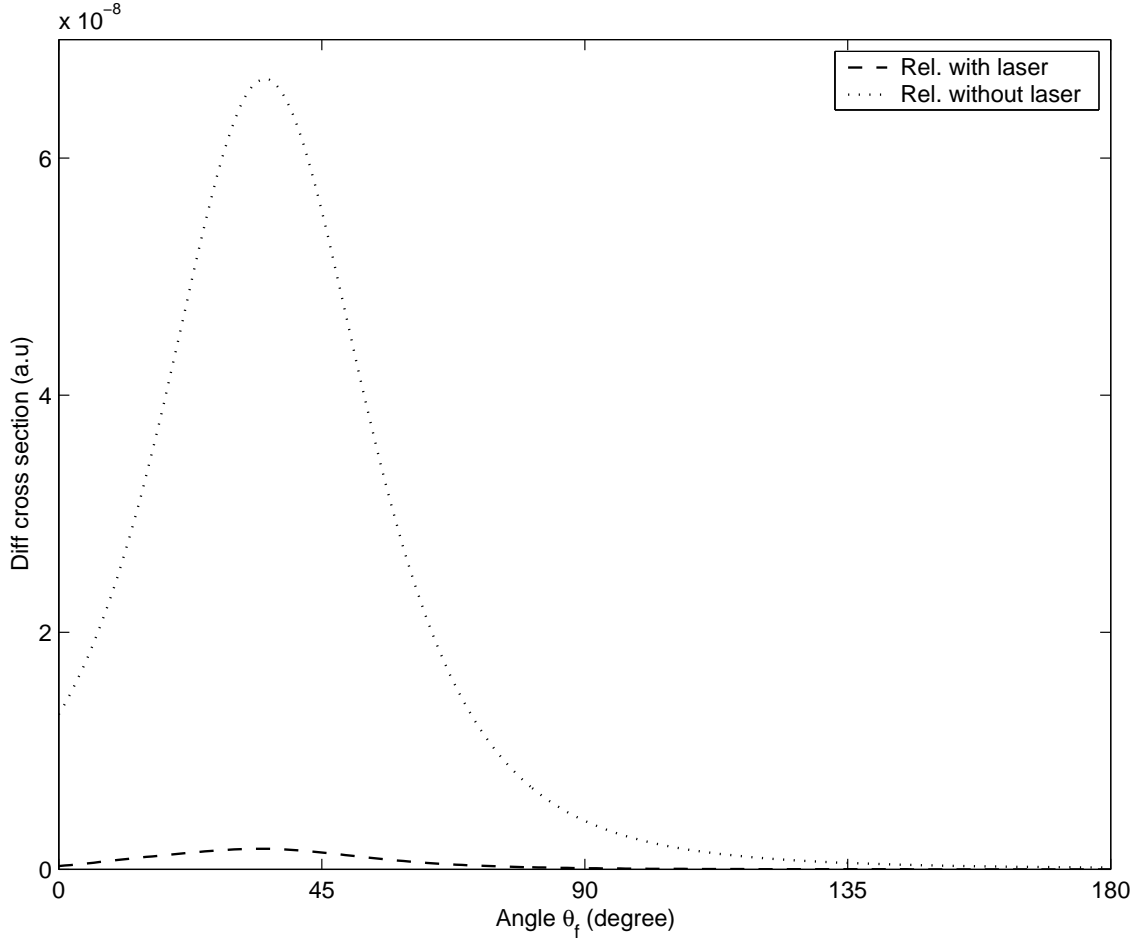


Figure 12: Comparison in the relativistic regime ( $\gamma = 2 a.u.$ ,  $\varepsilon = 1 a.u.$  and  $w = 0.043 a.u.$ ) between the relativistic DCS with laser and the relativistic DCS without laser for the exchange of  $\pm 3500$  photons. The geometry chosen is  $\theta_i = \phi_i = 45^\circ$  where  $\theta_f$  varies from  $0^\circ$  to  $180^\circ$  with  $\phi_f = 90^\circ$

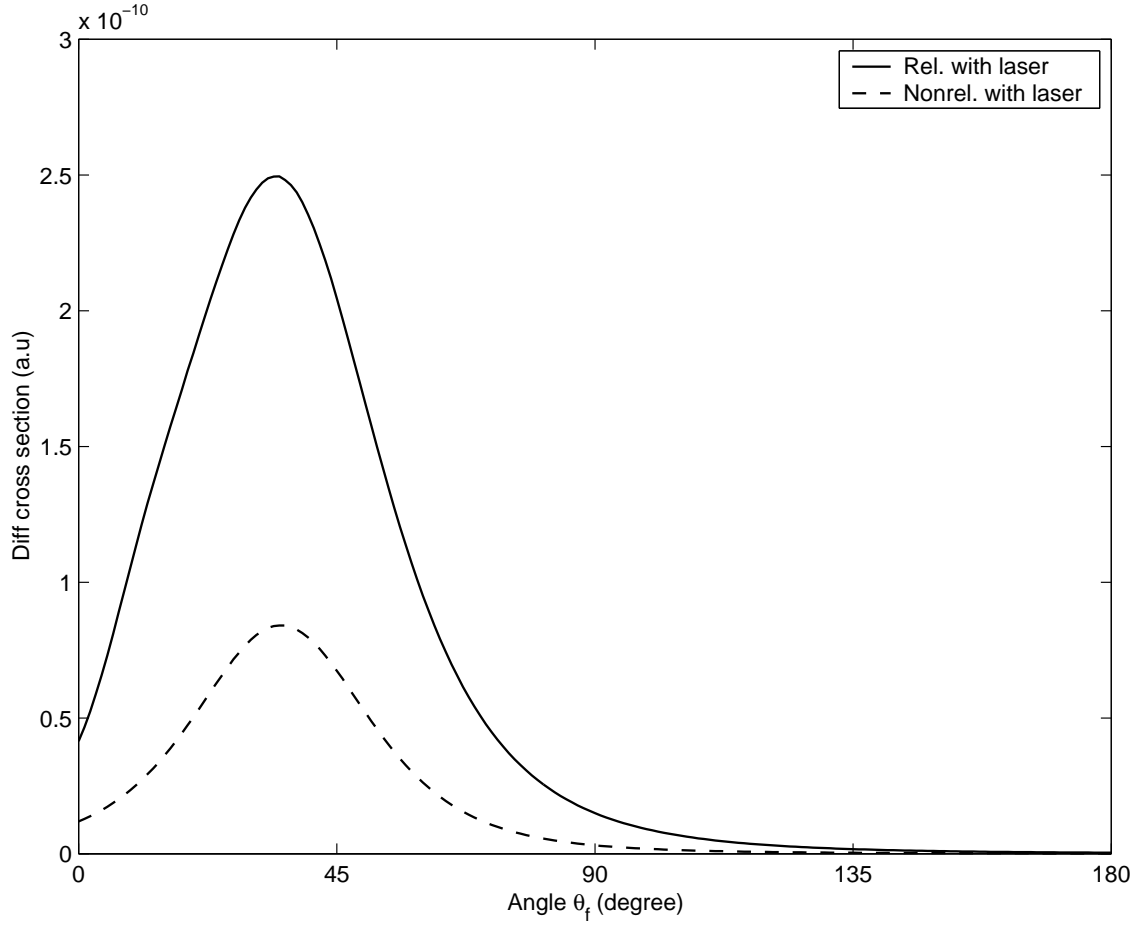


Figure 13: Comparison in the relativistic regime ( $\gamma = 2 a.u.$ ,  $\varepsilon = 1 a.u.$ ,  $w = 0.043 a.u.$ ) between the relativistic DCS with laser and the nonrelativistic DCS with laser for an exchange of  $\pm 500$  photons. The geometry chosen is  $\theta_i = \phi_i = 45^\circ$  where  $\theta_f$  varies from  $0^\circ$  to  $180^\circ$  with  $\phi_f = 90^\circ$



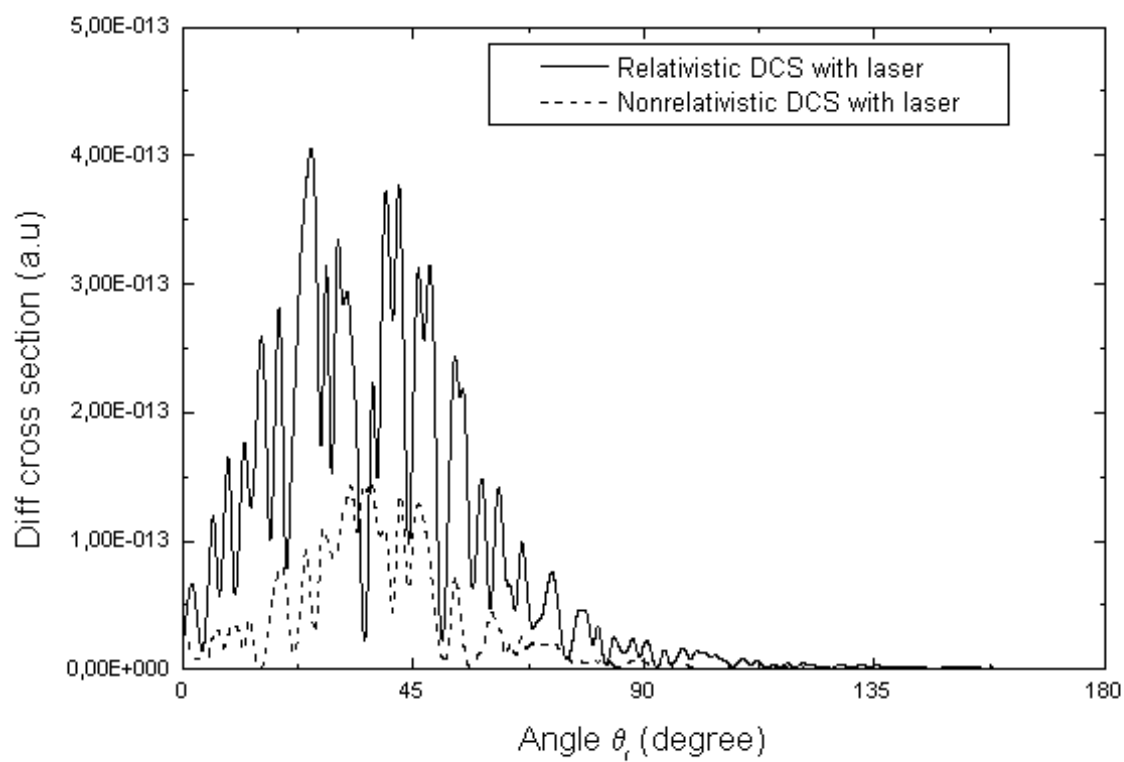


Figure 14: Comparison in the relativistic regime ( $\gamma = 2 a.u.$ ,  $\varepsilon = 1 a.u.$  and  $w = 0.043 a.u.$ ) between the relativistic DCS with laser and the nonrelativistic DCS with laser for absorption of one photon. The geometry chosen is  $\theta_i = \phi_i = 45^\circ$  where  $\theta_f$  varies from  $0^\circ$  to  $180^\circ$  with  $\phi_f = 90^\circ$

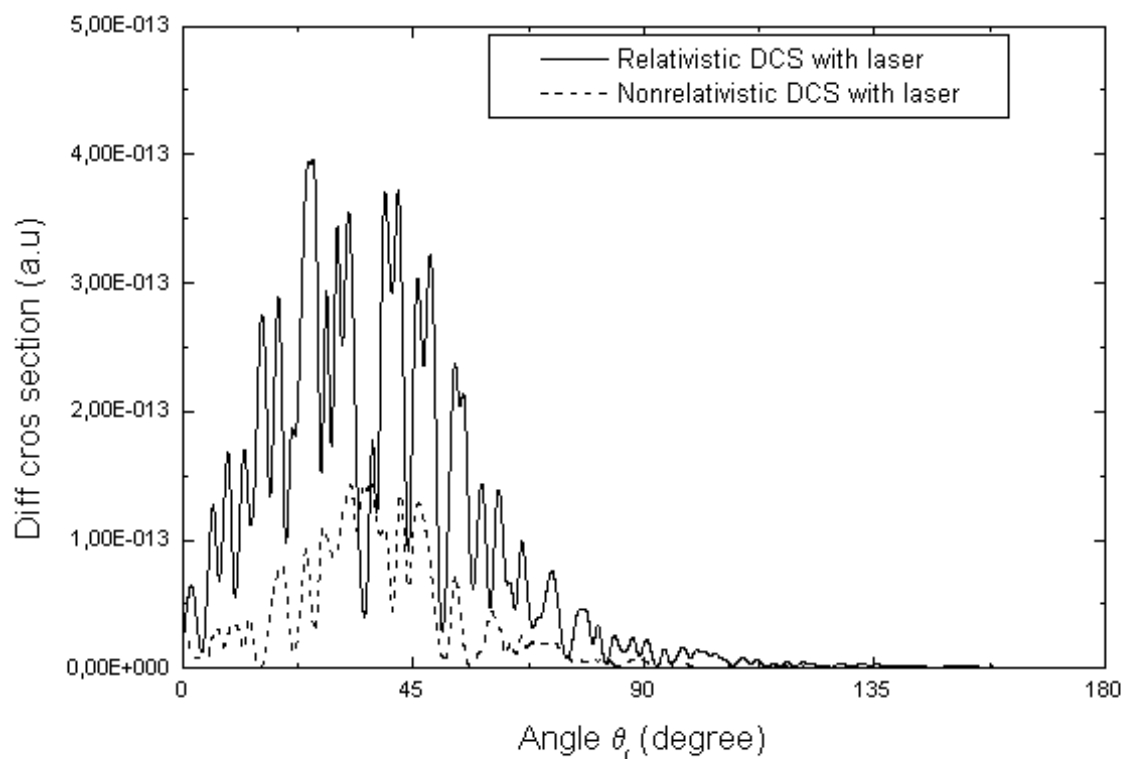


Figure 15: Comparison in the relativistic regime ( $\gamma = 2 a.u.$ ,  $\varepsilon = 1 a.u$  and  $w = 0.043 a.u$ ) between the relativistic DCS with laser and the nonrelativistic DCS with laser for emission of one photon. The geometry chosen is  $\theta_i = \phi_i = 45^\circ$  where  $\theta_f$  held of  $0^\circ$  to  $180^\circ$  with  $\phi_f = 90^\circ$ . The curves for absorption and emission are identical.

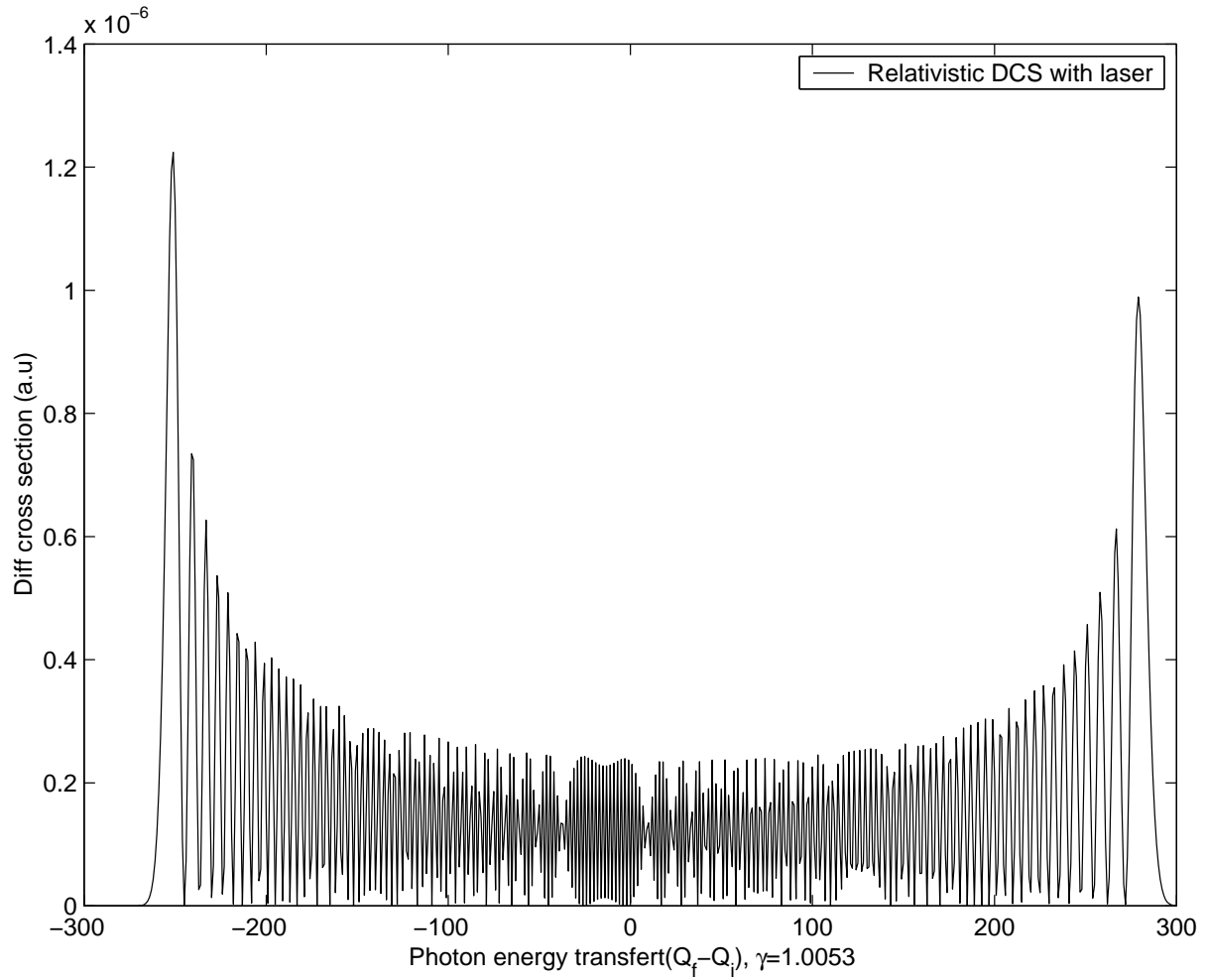


Figure 16: The envelope in the nonrelativistic regime ( $\gamma = 1.0053 a.u.$ ,  $\varepsilon = 0.05 a.u$  and  $w = 0.043 a.u$ ) of the relativistic DCS with laser for an exchange of  $\pm 300$  photons. The geometry chosen is  $\theta_i = \phi_i = 45^\circ$  where  $\theta_f = 90^\circ$  with  $\phi_f = 90^\circ$

$\cos(\theta(\mathbf{p}_i, \mathbf{p}_f))$	$\cos(\theta(\mathbf{q}_i, \mathbf{q}_f))$
0.862372	0.862049
0.863628	0.863303
0.864620	0.864294
0.865349	0.865022
0.865815	0.865487
0.866016	0.865688

**Table. 1** Comparison between some values of  $\cos(\theta(\mathbf{p}_i, \mathbf{p}_f))$  and  $\cos(\theta(\mathbf{q}_i, \mathbf{q}_f))$  in the nonrelativistic regime

$\cos(\theta(\mathbf{p}_i, \mathbf{p}_f))$	$\cos(\theta(\mathbf{q}_i, \mathbf{q}_f))$	
0.862372	0.851996	
0.863628	0.852976	
0.864620	0.853711	
0.865349	0.854200	
0.865815	0.854442	
0.866016	0.854438	

**Table. 2** Comparison between some values of  $\cos(\theta(\mathbf{p}_i, \mathbf{p}_f))$  and  $\cos(\theta(\mathbf{q}_i, \mathbf{q}_f))$  in the relativistic regime